Calorie Restriction Promotes Mitochondrial Biogenesis by Inducing the Expression of eNOS

Enzo Nisoli, *et al.*

Science **310**, 314 (2005);
DOI: 10.1126/science.1117728

Science (print ISSN 0036-8075; online ISSN 1095-9203) is published weekly, except the last week in December, by the American Association for the Advancement of Science, 1200 New York Avenue NW, Washington, DC 20005.

erable or few myosin heads are active. The ratio of one Rng3p per 50 myosin-II heads in the contractile ring (Table 1 and fig. S7) supports the latter hypothesis. In the temperature-sensitive *myo2-E1* mutant, the concentration of Rng3p is higher by threefold globally and ~60-fold in the contractile ring, perhaps to compensate for the minimal motor activity of this mutant (*14*). Large pools of most contractile-ring proteins remain in the cytoplasm during cytokinesis (Table 1) available for exchange with assembled rings, as observed in FRAP experiments (*38*, *39*).

The number of conventional myosin-II (Myo2p, Cdc4p, and Rlc1p) molecules in contractile rings is roughly constant from the time that a ring condenses through constriction (Fig. 3), so the local myosin concentration and force-producing capacity increase dramatically as the diameter of the ring declines. Cdc15p not only participates in ring assembly, but its number of molecules increases ~10-fold as rings mature during anaphase in preparations for septum formation. As rings constrict, the local concentrations of actin-binding proteins IQGAP Rng2p, Cdc15p, formin Cdc12p, and alpha-actinin Ain1p are nearly constant, so all are lost in proportion to the decline in the volume of ring. Septins Spn1p and Spn4p arrive late at the division site, forming rings with 15 to 22 μM septin that do not constrict as the septum forms (Fig. 3, C and D).

If used with caution, microscopy with fluorescent fusion proteins provides a precision measuring tool for quantitative biology. Our calibration method can be used to determine the concentration of any protein in yeast or other organisms with homologous recombination. Episomal expression of a YFP-fusion protein with measurement of the ratio of tagged and untagged proteins can be used where homologous gene replacement is impossible.

References and Notes

1. D. N. Robinson, G. Cavet, H. M. Warrick, J. A. Spudich, *BMC Cell Biol.* **3**, 4 (2002).
2. H. N. Higgs, T. P. Pollard, *J. Cell Biol.* **150**, 1311 (2000).
3. S. Ghaemmaghami *et al.*, *Nature* **425**, 737 (2003).
4. D. W. Piston, G. H. Patterson, S. M. Knobel, *Methods Cell Biol.* **58**, 31 (1999).
5. K. Hirschberg, R. D. Phair, J. Lippincott-Schwartz, *Methods Enzymol.* **327**, 69 (2000).
6. M. Dundr, J. G. McNally, J. Cohen, T. Misteli, *J. Struct. Biol.* **140**, 92 (2002).
7. J. Bähler *et al.*, *Yeast* **14**, 943 (1998).
8. J.-Q. Wu, J. R. Kuhn, D. R. Kovar, T. D. Pollard, *Dev. Cell* **5**, 723 (2003).
9. Materials and methods are available as supporting material on *Science* Online.
10. D. R. Kovar, J.-Q. Wu, T. D. Pollard, *Mol. Biol. Cell* **16**, 2313 (2005).
11. P. Nurse, P. Thuriaux, K. Nasmyth, *Mol. Gen. Genet.* **146**, 167 (1976).
12. M. Desautels, J. P. Den Haese, C. M. Slupsky, L. P. McIntosh, S. M. Hemmingsen, *J. Biol. Chem.* **276**, 5932 (2001).
13. V. M. D'Souza, N. I. Naqvi, H. Wang, M. K. Balasubramanian, *Cell Struct. Funct.* **26**, 555 (2001).
14. M. Lord, T. D. Pollard, *J. Cell Biol.* **167**, 315 (2004).
15. See the fission yeast handbook (available at www.sanger.ac.uk/PostGenomics/S_pombe/docs/nurse_lab_manual.pdf).
16. F. Sherman, *Methods Enzymol.* **350**, 3 (2002).
17. F. Chang, D. Drubin, P. Nurse, *J. Cell Biol.* **137**, 169 (1997).
18. M. Bezanilla, T. D. Pollard, *Mol. Biol. Cell* **11**, 79 (2000).
19. M. Anderson *et al.*, *EMBO J.* **21**, 5745 (2002).
20. J. J. Tasto, J. L. Morrell, K. L. Gould, *J. Cell Biol.* **160**, 1093 (2003).
21. C. Fankhauser *et al.*, *Cell* **82**, 435 (1995).
22. X. Peng *et al.*, *Mol. Biol. Cell* **16**, 1026 (2005).
23. G. Rustici *et al.*, *Nat. Genet.* **36**, 809 (2004).
24. V. Sirotkin, C. C. Beltzner, J.-B. Marchand, T. D. Pollard, *J. Cell Biol.* **170**, 637 (2005).
25. M. Kaksonen, Y. Sun, D. G. Drubin, *Cell* **115**, 475 (2003).
26. T. Takagi, S. A. Ishijima, H. Ochi, M. Osumi, *J. Electron Microsc.* **52**, 161 (2003).
27. M. E. Young, J. A. Cooper, P. C. Bridgman, *J. Cell Biol.* **166**, 629 (2004).
28. A. A. Rodal, L. Kozubowski, B. L. Goode, D. G. Drubin, J. H. Hartwig, *Mol. Biol. Cell* **16**, 372 (2005).
29. M. K. Balasubramanian, E. Bi, M. Glotzer, *Curr. Biol.* **14**, R806 (2004).
30. B. A. Wolfe, K. L. Gould, *Trends Cell Biol.* **15**, 10 (2005).
31. R. Ding, R. R. West, D. M. Morphew, B. R. Oakley, J. R. McIntosh, *Mol. Biol. Cell* **8**, 1461 (1997).
32. A. Grallert, A. Krapp, S. Bagley, V. Simanis, I. M. Hagan, *Genes Dev.* **18**, 1007 (2004).
33. J. L. Morrell *et al.*, *Curr. Biol.* **14**, 579 (2004).
34. J.-Q. Wu, T. D. Pollard, data not shown.
35. D. R. Kovar, T. D. Pollard, *Proc. Natl. Acad. Sci. U.S.A.* **101**, 14725 (2004).
36. R. H. Carnahan, K. L. Gould, *J. Cell Biol.* **162**, 851 (2003).
37. T. Kanbe, I. Kobayashi, K. Tanaka, *J. Cell Sci.* **94**, 647 (1989).
38. R. J. Pelham, F. Chang, *Nature* **419**, 82 (2002).
39. K. C. Y. Wong *et al.*, *Curr. Biol.* **12**, 724 (2002).
40. K. Nabeshima *et al.*, *Mol. Biol. Cell* **9**, 3211 (1998).
41. J. Bähler *et al.*, *J. Cell Biol.* **143**, 1603 (1998).
42. A. Paoletti, F. Chang, *Mol. Biol. Cell* **11**, 2757 (2000).
43. M. Sohrmann, C. Fankhauser, C. Brodbeck, V. Simanis, *Genes Dev.* **10**, 2707 (1996).
44. C. A. Blessing, G. T. Ugrinova, H. V. Goodson, *Trends Cell Biol.* **14**, 435 (2004).

45. We are grateful to M. Morphew and J. R. McIntosh for the generous gift of electron micrographs; K. L. Gould for Arp3p antibodies; J. Lessard for actin antibody; G. Law for help with the spinning disk confocal microscope; and M. Li, X.-Y. Wang, and T. Taylor for help with flow cytometry. We thank M. Manix and L. Zhao for some data analysis; C. Beltzner, D. Kovar, and M. Lord for yeast strains; D. Kovar and V. Sirotkin for actin plasmids; A. Downs for purified *S. pombe* actin; J. Kuhn, R. Mahaffy, and R. de Rooij for suggestions on microscopy and data analysis; and P. Forscher, P. Dalhaimer, D. Kovar, M. Lord, R. Mahaffy, and V. Sirotkin for comments on the manuscript. We are also grateful to other members of the Pollard laboratory for helpful suggestions. This work was supported by NIH Grant GM-26231 to T.D.P. and an Anna Fuller Fund Fellowship to J.-Q.W.

Supporting Online Material

www.sciencemag.org/cgi/content/full/310/5746/310/DC1
Materials and Methods
Figs. S1 to S7
Tables S1 and S2
References and Notes

6 April 2005; accepted 15 September 2005
10.1126/science.1113230

Calorie Restriction Promotes Mitochondrial Biogenesis by Inducing the Expression of eNOS

Enzo Nisoli,[1,2]* Cristina Tonello,[1] Annalisa Cardile,[1] Valeria Cozzi,[1] Renata Bracale,[1] Laura Tedesco,[1] Sestina Falcone,[1,3] Alessandra Valerio,[1] Orazio Cantoni,[4] Emilio Clementi,[1,3,5] Salvador Moncada,[6] Michele O. Carruba[1,2]

Calorie restriction extends life span in organisms ranging from yeast to mammals. Here, we report that calorie restriction for either 3 or 12 months induced endothelial nitric oxide synthase (eNOS) expression and 3′,5′-cyclic guanosine monophosphate formation in various tissues of male mice. This was accompanied by mitochondrial biogenesis, with increased oxygen consumption and adenosine triphosphate production, and an enhanced expression of sirtuin 1. These effects were strongly attenuated in eNOS null-mutant mice. Thus, nitric oxide plays a fundamental role in the processes induced by calorie restriction and may be involved in the extension of life span in mammals.

Calorie restriction (CR) extends life span in numerous organisms from yeast (*1*) to rodents and possibly primates (*2*). In mammals, CR delays the onset of age-associated diseases including cancer, atherosclerosis, and diabetes (*3*). A decrease in oxidative damage has been proposed as a mechanism (*4*); however, a lack of correlation between reactive oxygen species (ROS) production and life span was recently reported in *Drosophila* (*5*). Furthermore, increasing evidence suggests that SIRT1, the mammalian ortholog of the *SIR2* gene that mediates the life-extending effect of CR in yeast (*1*, *6*), is a key regulator of cell defenses and survival in mammals in response to stress (*7*).

Eight-week-old male wild-type mice were fed either ad libitum (AL) or with a CR diet (food provided on alternate days) for 3 or 12

[1]Integrated Laboratories Network, Department of Preclinical Sciences, Luigi Sacco Hospital, Milan University, 20157 Milan, Italy. [2]Istituto Auxologico Italiano, 20149 Milan, Italy. [3]Eugenio Medea Scientific Institute, 23842 Bosisio Parini, Italy. [4]Istituto di Farmacologia e Farmacognosia, University of Urbino "Carlo Bo," 61029 Urbino, Italy. [5]Stem Cell Research Institute, Dipartimento di Biotecnologie, Ospedale San Raffaele, 20132 Milan, Italy. [6]Wolfson Institute for Biomedical Research, University College London, London WC1E 6BT, UK.

*To whom correspondence should be addressed. E-mail: enzo.nisoli@unimi.it

months (*8*). Mice maintained on a CR feeding schedule consume 30 to 40% fewer calories over time compared with animals fed AL, have a lower body weight (fig. S1), and are known to have an extended life span (*9*). At 3 months of treatment, the amounts of mitochondrial DNA (mtDNA, a marker of mitochondrial content), the expression of peroxisome proliferator-activated receptor–γ coactivator 1α (PGC-1α), nuclear respiratory factor–1 (NRF-1), and mitochondrial transcription factor A (Tfam) [master regulators of mitochondrial biogenesis (*10*)], and expression of cytochrome c oxidase (COX-IV) and cytochrome c (Cyt c) (two mitochondrial proteins involved in cell respiration) were higher in white adipose tissue (WAT) and many other tissues of CR mice when compared with AL mice (Figs. 1A and 2A). This was consistent with increased mitochondrial biogenesis and mitochondrial gene expression (*11*–*13*).

To confirm that CR increases mitochondrial function, we measured oxygen consumption and expression of mitofusin (Mfn) 1 and 2 [the mitochondrial transmembrane guanosine triphosphatases crucial to the mitochondrial fusion process and metabolism (*14*, *15*)]. These parameters were higher in several tissues, particularly in WAT, of CR than in AL animals (Figs. 1, A and B, and 2). This suggests that CR induces mitochondrial biogenesis with increased respiration and expression of genes crucial for the dynamic fusion processes required for oxidative function. We then investigated whether the increase in respiration was associated with an increase in adenosine triphosphate (ATP) synthesis and found that CR increased ATP concentrations in WAT (0.025 ± 0.001 nmol/mg tissue in CR mice compared with 0.018 ± 0.002 nmol/mg tissue in AL mice, $P < 0.001$, $n = 4$ animals) and in other tissues (table S1). Similar results were obtained in mice treated for 12 months. Thus, the molecular changes induced by CR occur early and are long-lasting, consistent with the early onset and persistent effect of CR on life span (*9*).

Nitric oxide (NO) generated by eNOS increases mitochondrial biogenesis and enhances respiration and ATP content in various mammalian cells by acting through its second messenger, 3′,5′-cyclic guanosine monophosphate (cGMP) (*11*, *16*). We investigated whether eNOS and cGMP play a role in the mitochondrial biogenesis induced by CR. The expression of eNOS, unlike neuronal and inducible NOS, was higher in CR than in AL mice (Figs. 1A and 2) and was accompanied by higher concentrations of cGMP (Figs. 1C and 2) in WAT and in several other tissues. The increased serum concentrations of nitrite and nitrate (an index of NO production) and plasma cGMP in obese subjects exposed to CR in controlled weight loss trials (*17*, *18*) are consistent with our findings.

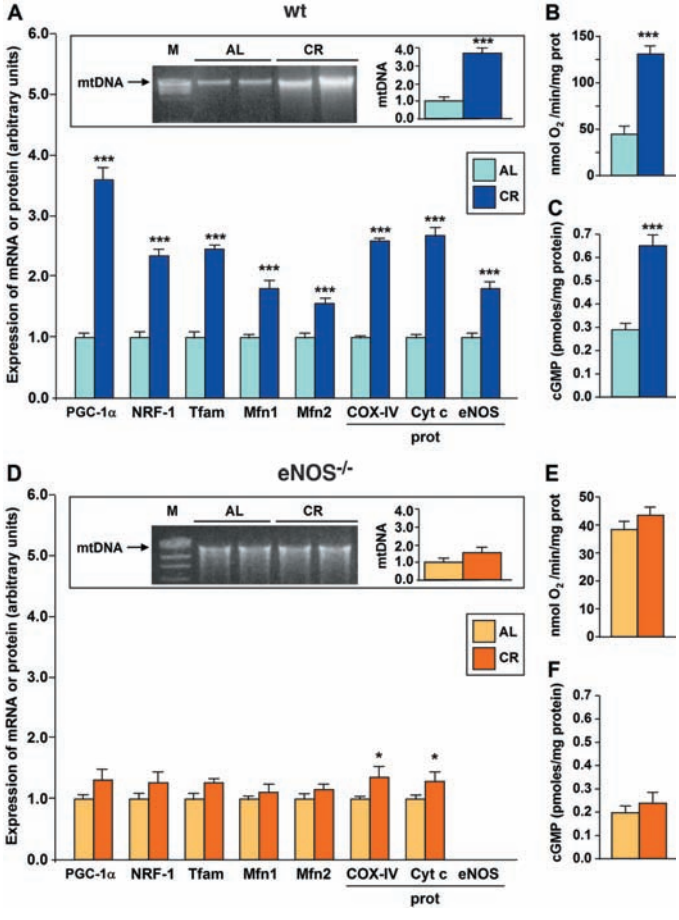

Fig. 1. CR induces mitochondrial biogenesis in WAT of wild-type (wt) but not eNOS$^{-/-}$ mice through eNOS expression and cGMP formation. (**A** and **D**) PGC-1α, NRF-1, Tfam, Mfn1, and Mfn2 mRNA were analyzed by means of quantitative reverse transcription polymerase chain reaction (RT-PCR); COX IV, Cyt c, and eNOS proteins were detected by immunoblot analysis. (Insets) WAT mtDNA (gel shows a representative experiment with two mice per group). The relative values were obtained by densitometric analysis, with those measured in the AL mice taken as 1.0. (**B** and **E**) O_2 consumption and (**C** and **F**) cGMP concentrations in WAT. Each experiment ($n = 10$) was repeated at least three times. Triple asterisks indicate $P < 0.001$, and single asterisk, $P < 0.05$, compared with AL-fed mice. Error bars indicate SEM.

To verify the role of eNOS in the mitochondrial biogenesis induced by CR, we fed 8-week-old male eNOS null-mutant (eNOS$^{-/-}$) mice either an AL or a CR diet for 3 months (Fig. 1, D to F, and fig. S2, A to C). In particular, mtDNA content and PGC-1α, NRF-1, Tfam, Mfn1, and Mfn2 mRNA amounts, although different from those in wild-type animals, were not significantly greater in CR eNOS$^{-/-}$ mice compared to in AL eNOS$^{-/-}$ animals. Moreover, COX IV and Cyt c expression did not increase significantly in CR animals except in WAT and brain, where these parameters increased to a much lesser extent than those in wild-type animals (Fig. 1D and fig. S2A). Thus, CR was unable to induce significant mitochondrial biogenesis in a number of tissues of eNOS$^{-/-}$ mice, including WAT. To confirm this, we measured oxygen consumption (Fig. 1E and fig. S2B) and cGMP (Fig. 1F and fig. S2C) and ATP concentrations (table S1) in WAT and other tissues (table S1) of both CR and AL eNOS$^{-/-}$ animals. These parameters also did not increase significantly as a result of CR in knock-out compared to in wild-type mice. AL eNOS$^{-/-}$ mice displayed greater feed efficiency (body weight gain per food intake) than their wild-type counterparts (*11*), suggesting that both energy expenditure and oxidative metabolism are partly NO-dependent. The CR wild-type mice showed lower feed efficiency values than AL wild-type animals (0.295 ± 0.023 compared with 0.488 ± 0.028, respectively; $P < 0.001$, $n = 10$ animals), whereas there was no difference between CR eNOS$^{-/-}$ mice and AL eNOS$^{-/-}$ animals (0.67 ± 0.025 and 0.654 ± 0.019, respectively; $n = 10$ animals). Thus, the CR-induced increase in oxidative metabolism appears to be blunted in the absence of eNOS expression in mammals.

Given the role of yeast SIR2 protein in life span extension by CR (*1*, *6*), we studied the expression of SIRT1 and found it to be higher in many tissues (fig. S3) of CR wild-type animals than of AL wild-type mice, including WAT (Fig. 3A) (*19*), where SIRT1 triggers lipolysis and loss of fat (*20*). SIRT1 mRNA and protein were ~threefold higher in cultured white adipocytes exposed either to NO donors, such as (Z)-1-[2-(2-aminoethyl)-N-(2-ammonioethyl)amino] diazen-1-ium-1,2 diolate (DETA-NO) and S-nitrosoacetyl penicillamine (SNAP), or to a cGMP analog (8 Br-cGMP) than in untreated cells (Fig. 3B) and ~80% lower in WAT of eNOS$^{-/-}$ mice when compared with wild-type animals (Fig. 3, C and D). Thus, the expression of SIRT1 in WAT during CR might be partly mediated by NO acting via cGMP.

To investigate whether the CR-induced SIRT1 expression was dependent on eNOS-derived NO, we performed immunoblot analysis in WAT of eNOS$^{-/-}$ mice fed either an AL or a CR diet. In eNOS$^{-/-}$ mice fed a CR diet, SIRT1 expression was also increased (~30%) in WAT compared with that of eNOS$^{-/-}$ mice

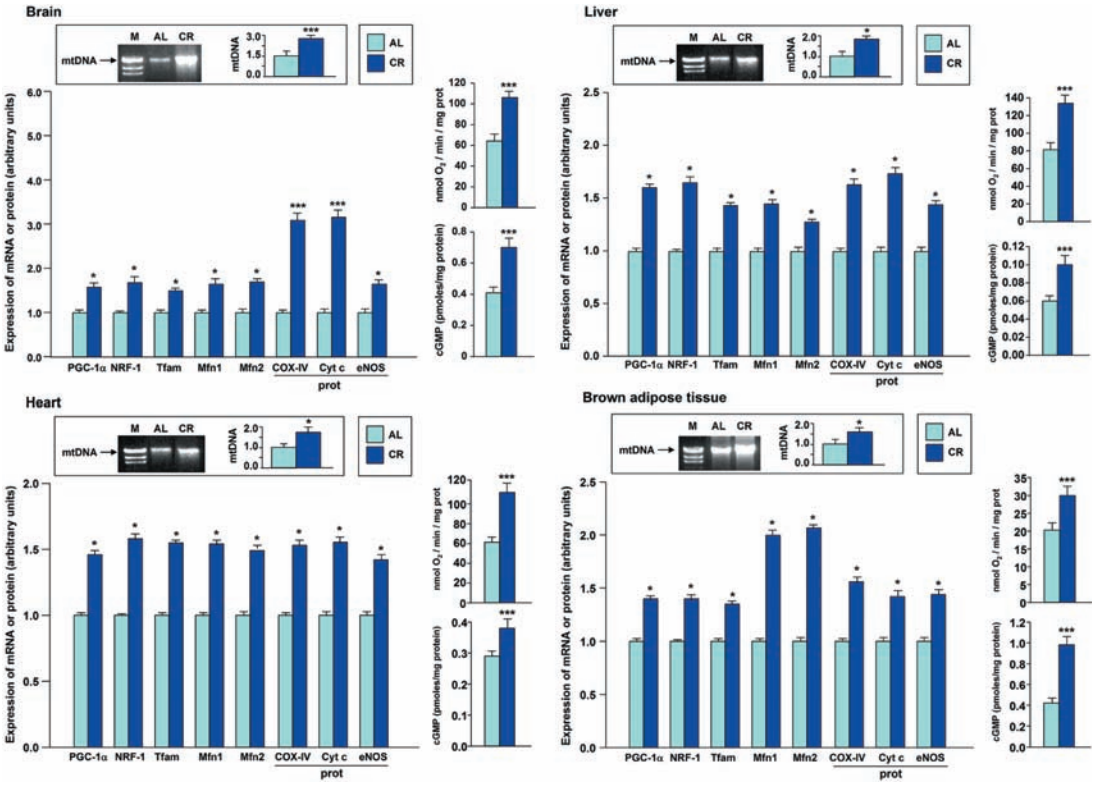

Fig. 2. CR induces mitochondrial biogenesis in different tissues of wt mice through eNOS expression and cGMP formation. (Large bar graphs) PGC-1α, NRF-1, Tfam, Mfn1, and Mfn2 mRNA were analyzed by means of quantitative RT-PCR with gene-specific oligonucleotide probes. COX IV, Cyt c, and eNOS proteins were detected by immunoblot analysis. (Top images) MtDNA (gel shows one representative experiment from one mouse per group). The relative values were obtained by densitometric analysis, with those measured in the AL mice taken as 1.0. (Top small bar graphs) O_2 consumption and (bottom small bar graphs) cGMP concentrations. Each experiment (n = 10 animals) was repeated at least three times. Triple asterisks, $P < 0.001$, and single asterisk, $P < 0.05$, compared with AL-fed mice. Error bars indicate SEM.

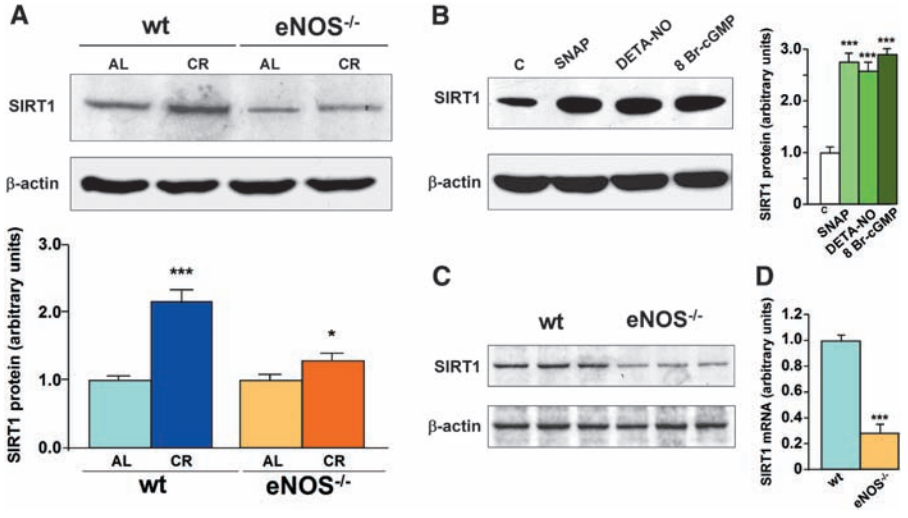

Fig. 3. SIRT1 expression is regulated by NO in WAT and white adipocytes. (**A**) SIRT1 protein levels in WAT of either AL or CR wt and eNOS$^{-/-}$ mice. A representative experiment is shown, with means ± SEM of densitometric measurements performed in 10 animals per group. The histogram values were obtained by densitometric analysis, with values measured in the AL mice taken as 1.0. (**B**) SIRT1 protein concentrations in white adipocytes cultured for 3 days with or without SNAP (100 μM), DETA-NO (50 μM), and 8 Br-cGMP (3 mM). A representative experiment is shown, with means ± SEM of densitometric measurements performed in five separate experiments. The protein concentrations were obtained by densitometric analysis, with values measured in the untreated cells (c) taken as 1.0. (**C** and **D**) SIRT1 protein and mRNA expression, respectively, in WAT of male eNOS$^{-/-}$ mice compared with wt mice. Each experiment (n = 10 animals) was repeated at least three times. The relative values of mRNA were obtained by densitometric analysis, with values measured in wt mice taken as 1.0. Triple asterisks, $P < 0.001$ and single asterisk, $P < 0.05$ compared with AL-fed wild-type mice or untreated cells.

fed an AL diet (Fig. 3A), although the change was much smaller than that in wild-type animals (~120%, $P < 0.001$). Similar results were obtained in the other tissues tested (fig. S3).

Thus, CR induces an increase in eNOS expression, which in turn is involved in both mitochondrial biogenesis and SIRT1 expression in a variety of tissues. The enhanced expression of SIRT1 by CR is consistent with a potential increase in life span. This transcription factor may be an evolutionarily ancient biological stress response that slows aging, promoting the mobilization of fat into the blood from WAT stores (*20*), the down-regulation of adipogenesis (*20*), and the long-term survival of irreplaceable cells (*7*, *19*). The increase in mitochondrial activity, i.e., in oxidative metabolism, that we see in CR animals is intriguing in view of the widely accepted hypothesis that CR increases longevity by slowing metabolism and reducing mitochondrial ROS and accompanying cellular damage (*4*). In fact, metabolic rate normalized to body weight does not decline in CR mice, and the lifetime metabolic output of these animals is therefore larger than that of their AL cohorts (*21*). Respiration actually increases during CR in yeast (*22*) and the nematode worm *Caenorhabditis elegans* (*23*). The effects of CR on life span may be independent of excessive ROS production.

The effects of CR in mammals are complex, affecting many organs and physiological pathways. Nevertheless, the significantly reduced effects observed in eNOS$^{-/-}$ animals point to a role for NO in the response to CR. eNOS$^{-/-}$ mice are characterized by a reduced life span (*24*) due to age-related diseases (*25*). One possibility is that in wild-type CR animals NO, acting via mitochondrial biogenesis and expression of SIRT1, increases β-oxidation and lipolysis. This would result in a reduction in the accumulation of fat, which is known to have an impact on life span (*26*, *27*).

References and Notes

1. S.-J. Lin, P.-A. Defossez, L. Guarente, *Science* **289**, 2126 (2000).
2. D. K. Ingram *et al.*, *Ann. N.Y. Acad. Sci.* **1019**, 412 (2004).
3. E. J. Masoro, *Exp. Gerontol.* **35**, 299 (2000).
4. R. S. Sohal, R. Weindruch, *Science* **273**, 59 (1996).
5. S. Miwa, K. Riyahi, L. Partridge, M. D. Brand, *Ann. N.Y. Acad. Sci.* **1019**, 388 (2004).
6. R. M. Anderson, K. J. Bitterman, J. G. Wood, O. Medvedik, D. A. Sinclair, *Nature* **423**, 181 (2003).
7. J. Luo *et al.*, *Cell* **107**, 137 (2001).
8. Materials and methods are available as supporting material on *Science* Online.
9. C. L. Goodrick, D. K. Ingram, M. A. Reynolds, J. R. Freeman, N. Cider, *Mech. Ageing Dev.* **55**, 69 (1990).
10. D. P. Kelly, R. C. Scarpulla, *Genes Dev.* **18**, 357 (2004).
11. E. Nisoli *et al.*, *Science* **299**, 896 (2003).
12. D. Larrouy, H. Vidal, F. Andreelli, M. Laville, D. Langin, *Int. J. Obes. Relat. Metab. Disord.* **23**, 1327 (1999).
13. Y. Higami *et al.*, *FASEB J.* **18**, 415 (2004).
14. T. Koshiba *et al.*, *Science* **305**, 858 (2004).
15. D. Bach *et al.*, *J. Biol. Chem.* **278**, 17190 (2003).
16. E. Nisoli *et al.*, *Proc. Natl. Acad. Sci. U.S.A.* **101**, 16507 (2004).
17. C. P. Fenster *et al.*, *Free Radic. Biol. Med.* **37**, 695 (2004).
18. P. Dessi-Fulgheri *et al.*, *Hypertension* **33**, 658 (1999).
19. H. Y. Cohen *et al.*, *Science* **305**, 390 (2004); published online 17 June 2004 (10.1126/science.1099196).
20. F. Picard *et al.*, *Nature* **429**, 771 (2004).
21. E. J. Masoro, B. P. Yu, H. A. Bertrand, *Proc. Natl. Acad. Sci. U.S.A.* **79**, 4239 (1982).
22. S. J. Lin *et al.*, *Nature* **418**, 344 (2002).
23. K. Houthoofd *et al.*, *Exp. Gerontol.* **37**, 1359 (2002).
24. E. Dere *et al.*, *Genes Brain Behav.* **1**, 204 (2002).
25. S. Cook *et al.*, *Swiss Med. Wkly.* **133**, 360 (2003).
26. M. Bluher, B. B. Kahn, C. R. Kahn, *Science* **299**, 572 (2003).
27. C. H. Chiu, W. D. Lin, S. Y. Huang, Y. H. Lee, *Genes Dev.* **18**, 1970 (2004).

28. We thank A. Higgs for help with the preparation of the manuscript, A. Marino for the early experiments of this research, and A. Mejetta for technical assistance. This work was supported by grants from the Ministero dell'Istruzione, dell'Università e della Ricerca cofinanziamento 2003, the Italian Ministry of Health, and the Italian Association of Cancer Research (AIRC).

Supporting Online Material

www.sciencemag.org/cgi/content/full/310/5746/314/DC1
Materials and Methods
Figs. S1 to S3
Table S1
References

21 July 2005; accepted 6 September 2005
10.1126/science.1117728

Sequence Variants in *SLITRK1* Are Associated with Tourette's Syndrome

Jesse F. Abelson,[1,2]* Kenneth Y. Kwan,[3,4]* Brian J. O'Roak,[2]* Danielle Y. Baek,[1,2] Althea A. Stillman,[2] Thomas M. Morgan,[2] Carol A. Mathews,[8] David L. Pauls,[9] Mladen-Roko Rašin,[3] Murat Gunel,[5] Nicole R. Davis,[1,2] A. Gulhan Ercan-Sencicek,[1,2] Danielle H. Guez,[2] John A. Spertus,[10] James F. Leckman,[1] Leon S. Dure IV,[11] Roger Kurlan,[12] Harvey S. Singer,[13] Donald L. Gilbert,[14] Anita Farhi,[7] Angeliki Louvi,[5] Richard P. Lifton,[2,6,7] Nenad Šestan,[3,4] Matthew W. State[1,2,4,6]†

Tourette's syndrome (TS) is a genetically influenced developmental neuropsychiatric disorder characterized by chronic vocal and motor tics. We studied *Slit and Trk-like 1* (*SLITRK1*) as a candidate gene on chromosome 13q31.1 because of its proximity to a de novo chromosomal inversion in a child with TS. Among 174 unrelated probands, we identified a frameshift mutation and two independent occurrences of the identical variant in the binding site for microRNA hsa-miR-189. These variants were absent from 3600 control chromosomes. *SLITRK1* mRNA and hsa-miR-189 showed an overlapping expression pattern in brain regions previously implicated in TS. Wild-type SLITRK1, but not the frameshift mutant, enhanced dendritic growth in primary neuronal cultures. Collectively, these findings support the association of rare *SLITRK1* sequence variants with TS.

TS is a potentially debilitating developmental neuropsychiatric disorder, characterized by the combination of persistent vocal and motor tics, that affects as many as 1 in 100 individuals (*1*, *2*). A substantial portion of clinically referred TS patients also suffer from obsessive-compulsive disorder (OCD), attention deficit hyperactivity disorder (ADHD), or depression (*3*). A TS spectrum of disorders that includes chronic vocal or motor tics as well as tic-related OCD and ADHD is widely recognized. Phenomenological and neurobiological evidence also supports the inclusion of some habit disorders, including trichotillomania (TTM), in this phenotypic spectrum (*4*, *5*).

Several decades of investigation have confirmed a substantial genetic contribution to TS (*6*). Early segregation analyses suggested that the disorder was inherited as a rare, autosomal dominant trait (*7*). However, more recent studies have supported poly- or oligogenic inheritance (*8*). Genome-wide analysis of linkage has implicated intervals on chromosomes 4, 5, 8, 11, and 17 (*9*–*12*), but to date no disease-related mutations have been identified. These investigations have been complicated by a phenotype that typically decreases in severity with age, a high population prevalence of transient tics, and symptoms that overlap with common disorders such as ADHD and OCD (*13*). In addition, marked locus heterogeneity, gene-environment interactions, and the further confounding of assortative mating (*14*, *15*) have all likely hindered gene-mapping efforts.

We focused on a rare subset of TS patients with chromosomal anomalies to circumvent some of these obstacles and identify candidate genes for intensive mutational screening. Such a strategy provides the opportunity to characterize functional sequence variants largely irrespective of their mode of inheritance. We identified a patient presenting with TS and ADHD and carrying a de novo chromosome 13 inversion, inv(13)(q31.1;q33.1) (*16*). There was no family history of tics, TS, OCD, TTM, or ADHD (Fig. 1). Genotyping with multiple short tandem repeat (STR) markers confirmed paternity (*16*) (table S1). The co-occurrence of a de novo chromosomal abnormality with the only known case of TS in the pedigree led us to fine map the rearrangement with the use of fluorescence in situ hybridization (FISH). We found that bacterial artificial chromosomes (BACs) RP11-375K12 and RP11-255P5 span the 13q31.1 and 13q33.1 breakpoints, respectively (Fig. 1, C to F, and table S2).

Three genes map within 500 kilobases (kb) of these two breakpoints (Fig. 1, E and F). Of these, *Slit and Trk-like family member 1* (*SLITRK1*), encoding a single-pass transmembrane protein with two leucine-rich repeat (LRR) motifs in its extracellular domain, was considered the strongest candidate for further study because of its

[1]Child Study Center, [2]Department of Genetics, [3]Department of Neurobiology, [4]Interdepartmental Neuroscience Program, [5]Department of Neurosurgery, [6]Center for Human Genetics and Genomics, [7]Howard Hughes Medical Institute, Yale University School of Medicine, New Haven, CT 06520, USA. [8]Department of Psychiatry, University of California–San Diego, San Diego, CA 92093, USA. [9]Psychiatric and Neurodevelopmental Genetics Unit, Massachusetts General Hospital, Harvard Medical School, Boston, MA 02114, USA. [10]Department of Medicine, University of Missouri–Kansas City, Kansas City, MO 64111, USA. [11]Division of Pediatric Neurology, Department of Pediatrics, University of Alabama at Birmingham, Birmingham, AL 35233, USA. [12]Department of Neurology, University of Rochester School of Medicine, Rochester, NY 14642, USA. [13]Departments of Neurology and Pediatrics, Johns Hopkins University School of Medicine, Baltimore, MD 21287, USA. [14]Division of Neurology, Cincinnati Children's Hospital Medical Center, Cincinnati, OH 45229, USA.

*These authors contributed equally to this work.
†To whom correspondence should be addressed. E-mail: matthew.state@yale.edu